Hybridization of *sd*- and *fp*-Shell Proton Orbitals in the System $^{36}S + ^{37}Cl$

R. Bilwes,[a] B. Bilwes, and L. Stuttge
Centre de Recherches Nucléaires, Strasbourg, France

J. L. Ferrero and J. A. Ruiz
Istituto de Fisica Corpuscular, Consejo Superior de Investigaciones Científicas, Universidad de Valencia, Valencia, Spain

W. von Oertzen[b]
Hahn-Meitner Institut, W-1000 Berlin 39, Germany

B. Imanishi
Institute for Nuclear Study, University of Tokyo, Tanashi, Tokyo 188, Japan
(Received 24 June 1992)

Experimental and theoretical evidence is presented that the proton exchange is strongly enhanced by a mixing of single-particle configurations in ^{37}Cl (in the system $^{36}S + ^{37}Cl$), which is shown to be the clearest example of hybridization in nuclear physics. The experimental data on elastic and inelastic transfer are only reproduced if the complete set of single-particle states ($d_{3/2}$, $s_{1/2}$, $f_{7/2}$, $p_{3/2}$, $f_{5/2}$, and $p_{1/2}$) is included in a coupled-reaction-channel calculation. The strong enhancement is explained by the hybridization of orbits of different parity. In a two-center molecular-orbital approach the density of the proton orbitals in the lowest state is shown to be concentrated at the center between the two ^{36}S cores.

PACS numbers: 24.10.Eq, 25.70.Bc, 25.70.Hi

Detailed experimental and theoretical studies in the past 5 years have shown increasing evidence of the importance of higher-order coupling effects in heavy-ion reactions at energies close to the Coulomb barrier [1]. Considerable improvement in experimental techniques and in computational means has allowed considerable progress in the quantitative understanding in this field. We present here data and an analysis where in a heavy-ion reaction involving nuclei of intermediate mass ($^{36}S + ^{37}Cl$) transitions to separated final states are observed, and a quantitative description of elastic scattering and transfer data was possible. The analysis based on known structural properties of the nuclei gives quantitative evidence for dynamical configuration mixing and the formation of molecular orbitals. The case $^{37}Cl + ^{36}S$ is particularly suitable because the valence protons in ^{37}Cl occupy states at the end of the *sd* shell and the first orbits of the *fp* shell. The mixing of orbits of different parity (*sd* and *fp*, known as hybridization [2,3]) gives a dramatic increase of the proton orbital density between the two cores and therefore a strong enhancement in the elastic transfer of the proton in the lowest orbit between the two ^{36}S cores.

The experimental data were obtained using the ^{37}Cl beam of the Strasbourg MP tandem accelerator. The targets consisted of ^{36}S (3 $\mu g/cm^2$) implanted in a thin ^{12}C foil. The kinematical coincidence technique was used to identify the reaction products and in order to obtain Q-value spectra [4]. The resolution of approximately 0.5 MeV allowed a clear separation of the ground-state transition and the single-particle excitations in ^{37}Cl at 1.73 MeV ($s_{1/2}$), 3.1 MeV ($f_{7/2}$), and 4.27 MeV ($p_{3/2}$); see Fig. 1. These states dominate in the transfer spectrum. In the intermediate angular region where the inelastic collective excitations of ^{36}S, the 2^+ state at 3.2 MeV, and the 3^- state at 4.19 MeV contribute, no separation from the corresponding single-particle states in ^{37}Cl ($f_{7/2}$ and $p_{3/2}$, respectively) is possible. At small angles, however, the collective excitations of ^{36}S dominate completely the angular distributions. The single-particle excitation of the ^{37}Cl states is only seen directly for the $s_{1/2}$ state. This discussion applies to the cross section of the ^{37}Cl nuclei written as $^{36}S(^{37}Cl, ^{37}Cl)^{36}S$. The differential cross sections are presented for the full angular range in Fig. 2, where the sum of the cross sections of different transitions

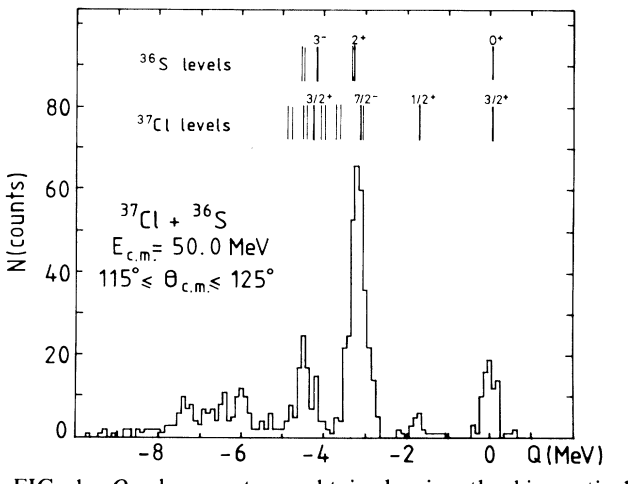

FIG. 1. Q-value spectrum obtained using the kinematical coincidence technique for the reaction $^{37}Cl + ^{36}S$ at $E_{c.m.} = 50$ MeV.

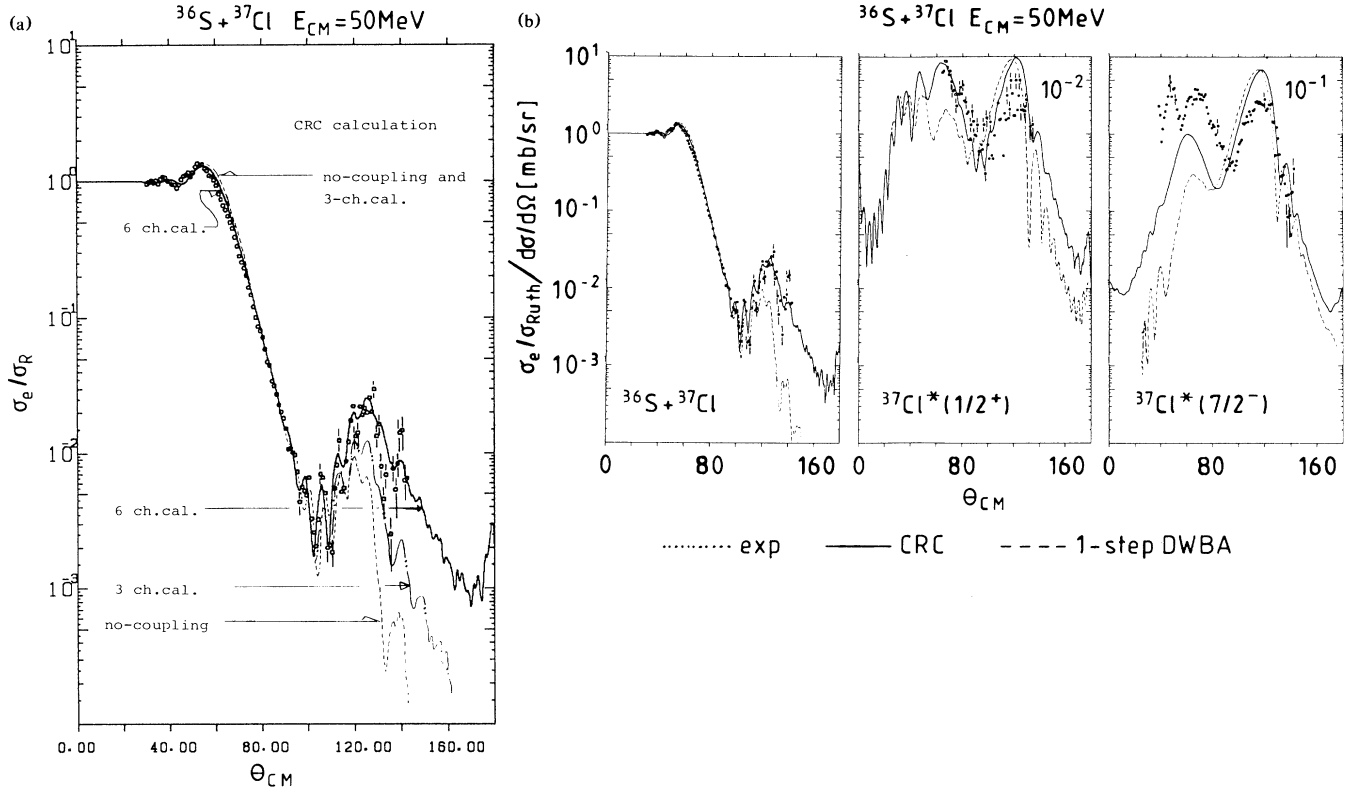

FIG. 2. (a) Differential cross sections for the elastic scattering in the scattering of $^{37}Cl+^{36}S$. The curves are CRC calculations with different numbers of basis states. Errors are given for some points in regions where they are larger than the dot symbols. (b) Same as (a) for the elastic scattering and the inelastic transitions in the $^{37}Cl+^{36}S$ system. The curves are complete (see also Table I) CRC calculations (solid lines) and one-step DWBA calculations (dashed lines), respectively.

as observed in the experiment is shown. The proton transfer $^{36}S(^{37}Cl,^{36}S)^{37}Cl$ appears as a backward rise for different states of ^{37}Cl. In the elastic channel oscillations arise from the interference of the elastic channel and the elastic transfer [5].

In Fig. 2 the experimental distributions are shown together with the analysis, presented by the solid lines. The calculation is based on a coupled-reaction-channel (CRC) approach, developed in recent years [3], where only single-particle states of the valence proton are included. Complete analysis, including excitations of the collective states of ^{36}S and using a different CRC code (FRESCO [6] by Thompson) will be presented elsewhere [7]; there we show that the inclusion of the collective states of ^{36}S mainly introduces a renormalization of the *core-core optical potential*. The latter is obtained by fits to the elastic scattering *with* the inclusion of the elastic transfer channel in all orders. The parameters of the present Woods-Saxon optical potential are $V=24.5$ MeV, $r_0=1.2$ fm, $a=0.78$ fm, $r_c=1.35$ fm (for the real part), and $W=7.0$ MeV, $r_i=1.35$ fm, $a_i=0.405$ fm (for the imaginary part). For the basis states a linear combination of single-center states with the known properties of the shell model configurations ($d_{3/2}$, $s_{1/2}$, $f_{7/2}$, $p_{3/2}$, $f_{5/2}$, and $p_{1/2}$) are chosen. The reaction proceeds through coherent superpositions of these states, which are induced by the interaction of the valence particle and the cores (^{36}S). The latter is obtained by the usual "shell model approach," where a binding potential of Woods-Saxon shape with parameters $r_0=1.25$ fm and $a_0=0.65$ fm is chosen and the depth adjusted (for each state) to reproduce the binding energies. From these values an average potential is chosen for both the positive and negative parity states.

In the analysis, we further need the spectroscopic strength of the transitions; the spectroscopic amplitudes of the proton states in ^{37}Cl are well known from reactions with light ions [8]. For the higher-lying orbits ($f_{7/2}$, $p_{3/2}$, $f_{5/2}$, and $p_{1/2}$) which are strongly fragmented, we chose only one state for each configuration with a strength which represents approximately 80% of the full strength. Therefore in the comparison with the data, where only one state is shown, the cross sections are overpredicted by approximately 50%. The relevant information is collected in Table I.

The CRC calculations reproduce the data very well if all configurations are included. In Fig. 2(a) we show the elastic transfer part (ground-state transition) with three

TABLE I. Binding energies (BE) and coefficients of fractional parantages (CFP) of the single-particle states in ^{37}Cl.

E_x (MeV)	g.s.	1.73	3.10	4.80	6.80	8.40
Config.	$d_{3/2}$	$s_{1/2}$	$f_{7/2}$	$p_{3/2}$	$p_{1/2}$	$f_{5/2}$
BE (MeV)	8.40	6.67	5.30	3.60	1.60	0.005
CFP	1.0	0.65	0.80	0.90	0.90	0.90

different calculations; the first contains only one channel ($d_{3/2}$), for the second three channels ($d_{3/2},s_{1/2},f_{7/2}$) are included, and finally six channels are used as indicated in Table I. The elastic transfer cross section is strongly influenced by the inclusion of higher orbits. A strong coupled-channel effect is observed with the inclusion of six channels. The cross sections for other single-particle states are also affected as shown in Fig. 2(b), where angular distributions for the measured single-particle states are shown. The solid line is for the case of the full calculation and the dashed curve is for the one-step distorted wave Born approximation (DWBA) treatment of the transitions to the excited states. The large CRC effects become evident in all channels. A typical effect for all transfer channels is a shift of the angular distributions to smaller angles [larger angles, if plotted as $180°-\theta_{\mathrm{c.m.}}$, as is the case for the proton transfer ^{36}S(^{37}Cl,^{36}S)^{37}Cl]. This indicates contributions from larger distances of the cores, which are made possible by a distortion of the nucleonic orbitals.

The origin of the changes in the angular distributions with the inclusion of the higher single-particle orbits can be analyzed by using the rotating molecular orbital approach [3]. In this approach the two-center wave functions are created by a linear combination of nuclear orbitals (LCNO) [5]. These two-center wave functions, for a basis which contains the single-center orbitals as given in Table I, are diagonalized for an intrinsic Hamiltonian which contains the core-valence nucleon interactions *and* the rotational terms from the relative motion. These rotating molecular orbitals (RMO) [3] with quantum numbers J,π,P represent the intrinsic configurations of the valence nucleon in the system. The RMO are classified according to the total angular momentum J, the parity π, and a counting index P ($P=1$ for the lowest state). The Coriolis interaction mixes states of different quantum number K (projection of the total angular momentum on the two-center axis), which is no longer a conserved quantum number. Thus, in addition, an index P is needed which labels the mixed two-center states. Mixing of configurations is induced by transfer and direct interactions. It sets in at rather large distances depending on binding energies and other properties of single-particle states. The intrinsic RMO states have eigenenergies which depend on the internuclear distance, which in an adiabatic case (for example, for the lowest state) can be interpreted as an additional potential term to the core-core interaction. We find that the lowest state, with index $P=1$, is an almost pure $K=\frac{1}{2}$ state in the grazing region for positive parity, and gains a considerable amount of energy, which in the barrier region corresponds already to 2–3 MeV. This strong effect guarantees that the lowest molecular-orbital state satisfies the adiabatic condition, showing in fact a stable configuration, and it determines the behavior of the elastic channel. A more close inspection of the coupling diagrams and of the density distribution of all substates shows that the ground state collects the major part of the proton density at the center between the two nuclei and causes a dramatic increase of density of the protons between the two cores as shown below (Fig. 3).

For a further discussion of the effects introduced by the coupling we can inspect the density distribution of the proton in the lowest two-center orbital. Figure 3 shows densities at a two-center distance which are slightly smaller than the barrier radius and for $J^{\pi}=\frac{63}{2}^{+}$ (this value corresponds to the relevant grazing angular momentum). Figure 3 shows the calculated proton density for (a) a simple superposition of the $d_{3/2}$ orbits of the two centers, (b) the density for the mixed state, when the $s_{1/2}$ and $f_{7/2}$ configurations are included, and (c) the full configuration space. The horizontal axis is given along the distance between the two ^{36}S cores. The vertical axis is subdivided into sixteen colors in a linear scale, with a relative normalization indicated for each figure.

With the inclusion of the $f_{7/2}$ state in case (b), the effect of the mixing of two states with opposite parity becomes apparent. It induces a dramatic increase of the density at the center between the two cores; the effect is further enhanced if the other configurations of the fp shell are included [case (c)]. These density plots show clearly the effect of *hybridization*, which is responsible for the corresponding changes in the angular distributions.

To summarize our result, we can state that the present case is the clearest example of hybridization in nuclear physics. Other examples which are connected to the mixing of the p and sd shells in the interactions involving ^{13}C are discussed extensively in Ref. [3]. Future reaction studies involving radioactive beams (e.g., ^{13}N or ^{11}Be) will clearly show manifestations of this basic quantum-mechanical effect, because it will be strongly enhanced for loosely bound (and quasibound) nucleon orbits. A large increase in these effects will be connected to the po-

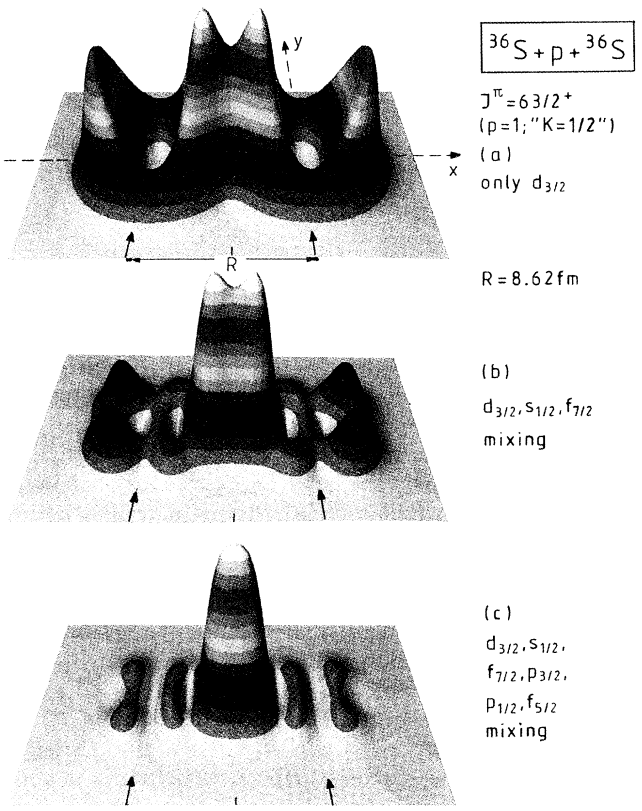

FIG. 3. Density distributions of the valence proton in the lowest state (with $J^{\pi}=\frac{63}{2}^{+}$) for different steps of configuration mixing. The strong asymmetric distortion (hybridization) is due to the mixing of opposite-parity shells (*sd* and *fp*). The two lowest points in the depression (at $\pm R/2$) in (a) mark the position of the two nuclear cores. The distance of $R=8.64$ fm is at the barrier radius ($r_{0B}=1.35$ fm, $R_B=8.9$ fm). The distributions in the different figures are renormalized to give the same maximum magnitude in the color scale (sixteen colors in a linear scale). The relative scaling factors for each figure are as follows: (a) only $d_{3/2}$ orbits, scaling 1.0; (b) $d_{3/2}$, $s_{1/2}$, and $f_{7/2}$ orbits included, downscaled by a factor of 2.2; (c) all configurations included ($d_{3/2}$, $s_{1/2}$, $f_{7/2}$, $p_{3/2}$, $p_{1/2}$, and $f_{5/2}$ orbits), downscaled by a factor of 5.08.

larizability of nucleon orbits with weak binding and the occurrence of strong low-lying $E1$ transitions [9] in cases of nucleon orbits with large radial extension. Further, the interaction of heavy nuclei in the vicinity of the Coulomb barrier [10,11], where cold multinucleon transfer reactions occur and give rise to the formation of a neck between the two nuclei, will be strongly influenced by hybridization. This is particularly relevant because the strong spin-orbit splitting in nuclei causes the orbits of the next main shell to approach the valence shells of the interacting nuclei. Nuclei which are unstable to octupole deformation deserve special attention, because here again the parity mixing of nucleon orbits becomes possible [12]. Strong coupled-channel effects can therefore be anticipated in interactions of weakly bound nuclei (using radioactive beams), if the valence orbits of the nucleons are in the vicinity of a closed shell where hybridization can occur. Further advances in experimental techniques and computational means will thus uncover a rich field of two-center problems in nuclear physics.

The authors are indebted to A. von Oertzen for his help in producing Fig. 3. One of the authors (W.v.Oe.) expresses his gratitude to CRN, Strasbourg, for the hospitality extended to him in 1990. Two of the authors (W.v.Oe., B.I.) acknowledge the support of the Foundation of Japanese Society of Promotion of Sciences (JSPS).

[a]Deceased.
[b]Also at Fachbereich Physik, Freie Universität, Berlin, Germany.

[1] *Heavy Ion Collisions at Energies near the Coulomb Barrier*, edited by M. A. Nagarajan, IOP Conf. Proc. No. 110 (Institute of Physics, London, 1990).
[2] L. Pauling, *The Nature of the Chemical Bond* (Cornell Univ. Press, Ithaca, 1960).
[3] B. Imanishi and W. von Oertzen, Phys. Rep. **155**, 29 (1987).
[4] L. Stuttge, these, Université de Strasbourg, 1985; B. Bilwes, R. Bilwes, V. D'Amico, J. L. Ferrero, R. Potenza, and G. Giardina, Nucl. Phys. **A408**, 173 (1983).
[5] W. von Oertzen and H. G. Bohlen, Phys. Rep. **19**, 1 (1975).
[6] I. A. Thompson, computer code FRESCO (private communication); Comput. Phys. Rep. **167**, 7 (1988).
[7] B. Bilwes and W. von Oertzen (to be published).
[8] P. M. Endt and C. van der Leun, Nucl. Phys. **A310**, 1 (1978).
[9] T. Uchivyama and H. Morinaga, Z. Phys. A **320**, 273 (1985).
[10] M. Wilpert, B. Gebauer, W. von Oertzen, Th. Wilpert, E. Stiliaris, and H. G. Bohlen, Phys. Rev. C **44**, 1081 (1991).
[11] P. H. Stelson, in *Heavy Ion Collisions at Energies near the Coulomb Barrier* (Ref. [1]), p. 191.
[12] W. Nazarewicz, Nucl. Phys. **A520**, 333c (1991).

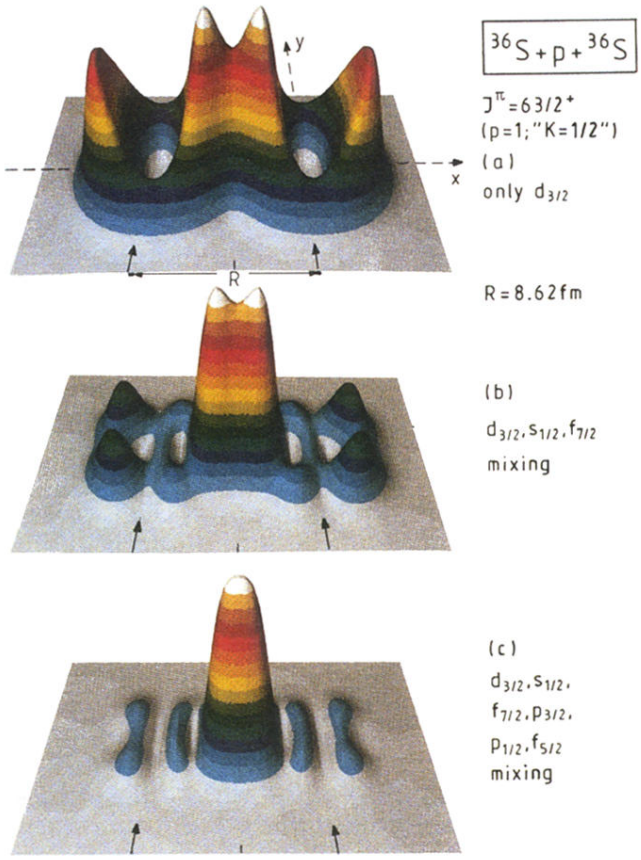

FIG. 3. Density distributions of the valence proton in the lowest state (with $J^{\pi} = \frac{63}{2}^{+}$) for different steps of configuration mixing. The strong asymmetric distortion (hybridization) is due to the mixing of opposite-parity shells (sd and fp). The two lowest points in the depression (at $\pm R/2$) in (a) mark the position of the two nuclear cores. The distance of $R = 8.64$ fm is at the barrier radius ($r_{0B} = 1.35$ fm, $R_B = 8.9$ fm). The distributions in the different figures are renormalized to give the same maximum magnitude in the color scale (sixteen colors in a linear scale). The relative scaling factors for each figure are as follows: (a) only $d_{3/2}$ orbits, scaling 1.0; (b) $d_{3/2}$, $s_{1/2}$, and $f_{7/2}$ orbits included, downscaled by a factor of 2.2; (c) all configurations included ($d_{3/2}$, $s_{1/2}$, $f_{7/2}$, $p_{3/2}$, $p_{1/2}$, and $f_{5/2}$ orbits), downscaled by a factor of 5.08.